analytical chemistry

pubs.acs.org/ac
Article

Chromophore Optimization in Organometallic Au(III) Cys Arylation of Peptides and Proteins for 266 nm Photoactivation

Jacob W. Silzel, Chengwei Chen, Colomba Sanchez-Marsetti, Phillip Farias, Veronica Carta, W. Hill Harman, and Ryan R. Julian*

Cite This: *Anal. Chem.* 2024, 96, 14581−14589
Read Online

ACCESS | Metrics & More | Article Recommendations | Supporting Information

ABSTRACT: Cysteine is the most reactive naturally occurring amino acid due to the presence of a free thiol, presenting a tantalizing handle for covalent modification of peptides/proteins. Although many mass spectrometry experiments could benefit from site-specific modification of Cys, the utility of direct arylation has not been thoroughly explored. Recently, Spokoyny and co-workers reported a Au(III) organometallic reagent that robustly arylates Cys and tolerates a wide variety of solvents and conditions. Given the chromophoric nature of aryl groups and the known susceptibility of carbon−sulfur bonds to photodissociation, we set out to identify an aryl group that could efficiently cleave Cys carbon−sulfur bonds at 266 nm. A streamlined workflow was developed to facilitate rapid examination of a large number of aryls with minimal sample using a simple test peptide, RAAACGVLK. We were able to identify several aryl groups that yield abundant homolytic photodissociation of the adjacent Cys carbon−sulfur bonds with short activation times (<10 ms). In addition, we characterized the radical products created by photodissociation by subjecting the product ions to further collisional activation. Finally, we tested Cys arylation with human hemoglobin, identified reaction conditions that facilitate efficient modification of intact proteins, and evaluated the photochemistry and activation of these large radical ions.

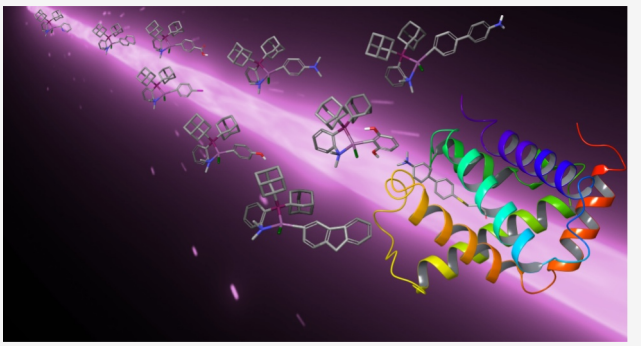

INTRODUCTION

Recent advances in both mass spectrometry and lasers have enabled the development of powerful new platforms for protein analysis. Fragmentation of peptides/proteins with far UV light, a method frequently called ultraviolet photodissociation or UVPD, generates a wide variety of fragments via a combination of dissociative electronic excitation and internal conversion into vibrational energy.[1,2] While collisional activation tends to generate mainly b/y backbone fragments, UVPD produces more varied fragmentation including a/x, c/z, and b/y backbone fragments, as well as ±1 or 2 Da species for many of these fragments.[3,4] Cleavage of C−S and S−S bonds is also favored in UVPD to varying extents depending on the incident wavelength.[5,6] The extensive backbone dissociation following photoactivation at 193 or 157 nm can be used to obtain high sequence coverage when characterizing peptides and proteins.[7,8] More recently, 213 nm has also been introduced for UVPD experiments.[9] Although 213 nm photons are just outside the far UV and the predicted absorption for peptides and proteins is lower compared to 193 or 157 nm, similar results are obtained when implemented in actual proteomics experiments.[3]

266 nm Chromophores. While UVPD of unmodified peptides and proteins is limited to higher energy wavelengths such as 213 or 193 nm, derivatization of biomolecules with appropriate chromophores enables more selective absorption of photons at longer wavelengths that normally would not induce significant fragmentation. This approach has been explored for both proteins and lipids, utilizing a wide variety of reagents such as nitroazobenzene or acetophenone.[10,11] At a slightly longer wavelength and lower energy, 266 nm photons do not contain sufficient energy to access dissociative excited states along the peptide backbone. In fact, outside of the side chains of Trp, Tyr, and Phe, absorption at 266 nm essentially does not occur in proteins. As a consequence, excitation of unmodified peptides and proteins with 266 nm photons typically results in very little dissociation. However, 266 nm photons can access dissociative excited-state chemistry for bonds that are not native to peptides and proteins. For example, 266 nm light has been used to selectively and homolytically cleave C−I bonds to create hydrogen deficient

Received: June 11, 2024
Revised: August 20, 2024
Accepted: August 22, 2024
Published: August 28, 2024

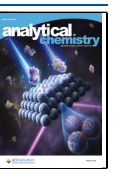

radicals for radical-directed dissociation (RDD).[12] The process of RDD involves reisolation and collisional activation of the radical created during 266 nm PD, facilitating radical migration and fragmentation (typically by a favorable beta-dissociation mechanism). RDD fragmentation usually occurs at lower energy than that required for mobile proton-driven b/y ion fragmentation.[13] RDD also generates different fragment ion types, including a/x and c/z backbone fragments as well as type I and II residue-specific side chain losses resulting in either full or partial loss of specific amino acid side chains depending on whether the radical attacks the alpha or gamma position.[14]

RDD requires the addition of a suitable radical precursor. Ideally, the chromophore should selectively dissociate to give a high yield of radical at 266 nm and should also be easily attached in high yields at specific residues. Most previous work has focused on C−I bond dissociation by installation of covalent or noncovalent modifications involving lysine or the N-terminus,[15,16] or iodination of Tyr.[17] However, intriguing results have also been obtained by C−S bond cleavage after phosphorylated Ser/Thr residues were modified to mimic Cys following β elimination and subsequent Michael addition with naphthalene thiol.[18] Unfortunately, phosphorylated Ser/Thr is not typically abundant, and even when present, the modification chemistry results in low yields. Cys itself is also an attractive target for site-selective modification due to its unique reactivity[19,20] and relative scarcity (Cys only comprises about 2.3% of the amino acids in the human proteome).[21] Quinone-based modification of Cys via Michael addition proceeds readily, but quinone modifications exhibit modest photoactivity and there are limited options for optimizing the chromophoric properties further.[22] At the time of this previous work, alternate pathways involving direct arylation of Cys itself had not been reported, a circumstance that is no longer true.

Arylation of Peptides. Several strategies have now been reported for direct Cys arylation employing transition metal catalysis.[23,24] In particular, recent organometallic gold(III) catalyzed arylation reported by Spokoyny and co-workers (see Scheme 1a and b) is appealing due to the specificity and broad functional group tolerance of the modification chemistry.[25,26] These modifications proceed quickly, can be performed at ambient temperatures, work well over a wide pH range, can be performed in many different solvents, and utilize aryl iodide precursors for which there are a significant number of commercially available options. In addition, the Au(III) compounds and Au(I) byproducts exhibit little reactivity with other functional groups found in peptides and proteins, which should limit the formation of side products.[27] This chemistry has opened many new avenues of peptide chemistry to be explored, such as allowing stapling of peptides, creation of peptide bicycles, construction of entire nanoassemblies of multiple peptides conjugated together, or facile conjugation of PEG to large biomolecules.[27,28] With this in mind, the ability of Au(III)-based reagents to rapidly arylate free thiols in peptides and proteins is of great interest to RDD, as new chromophores could open up the potential for new radical fragmentation pathways as well as provide another handle by which a 266 nm radical precursor could be covalently introduced into a biomolecule of interest (Scheme 1c).

In this work, we developed and applied an expedited reaction workflow to rapidly screen a wide variety of aryl iodides for 266 nm photoactivity and RDD suitability. Utilizing the isolation, separation, and characterization power of mass spectrometry (MS), we were able to significantly reduce the scale and time required to generate and evaluate candidate chromophores. Our screening led to identification of an aryl addition that produces C−S bond cleavage in yields similar to the best C−I bond photochemistry reported previously. Interestingly, this aryl contains a fixed charge, contrasting any previous chromophores used for RDD. The RDD behavior of this new aryl was tested on several peptides and a mixture of alpha- and beta-hemoglobin.

Scheme 1. Synthesis of (Me-DalPhos)Au(Aryl)Cl Complexes (a), Arylation of Thiol-Containing Peptides (b), and (c) 266 nm Photodissociation of Arylated Peptide and Subsequent Radical Migration Based on Previous Work with Analogous Modified Cysteines[18,22]

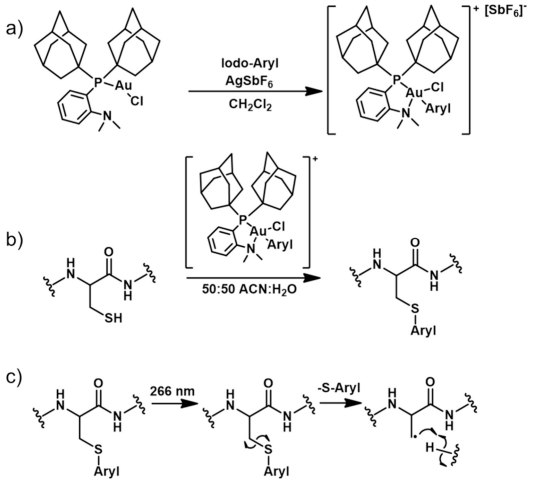

EXPERIMENTAL SECTION

Materials. Organic solvents and reagents were purchased from Fisher Scientific, Sigma-Aldrich, or Acros and used without further purification. FMOC-protected amino acids and Wang resins were purchased from Anaspec, Inc. or Chem-Impex International. Tau fragments (VQIVY KPVDL SKVTS KCGSL GNIHH KPGGG Q) and (VQIIN KKLDL SNVQS KCGSK DNIKH VPGGG S) were purchased from BACHEM. RAAACGVLK was synthesized via a solid-phase peptide synthesis. Iodo-aryl compounds (2-iodopyridine, 3-iodopyridine, 4-iodopyridine, 2-iodoaniline, 4-iodoaniline, 4-Iodo-N,N-dimethylaniline, 3-iodophenol, 4-iodophenol, 4-iodobenzoic acid, 4-iodo benzamide, 1-iodo-4-nitrobenzene, 2-iodoresorcinol, 2-iodonaphthalene, 2-iodobiphenyl, 4′-Iodo-(1,1′-biphenyl)-4-amine, 4′-iodo-N,N-dimethyl-[1,1′-biphenyl]-4-amine, 4-iodobenzenesulfonic acid, 1-iodo-2-naphthol, 4-iodobenzylamine, 2-iodo-m-xylene, iodo-4-(4-phenyl)-pyridine, and 2-iodo-9H-fluorene) were purchased from Fisher Scientific, Sigma-Aldrich, Ambeed, Honeywell, and Asta Tech. Di(1-adamantyl)-2-dimethylaminophenylphosphine (Me-DalPhos), silver hexafluoroantimonate, methyl iodide, and human hemoglobin were purchased from Sigma-Aldrich.

Synthesis of Iodo-biphenyl Quaternary Amine. (4′-Iodobiphenyl-4-yl) amine (21.4 mg) was dissolved in 1 mL of dry acetone in a flame-dried glass vial. 2,6-Lutidine was added in a 1:1 molar ratio, and a stir bar was added to mix the reaction. Methyl iodide was diluted in dry acetone, and 5× 100 μL aliquots were spaced 10 min apart (30-fold excess total) and were added to the reaction while stirring at room

https://doi.org/10.1021/acs.analchem.4c03001
Anal. Chem. 2024, 96, 14581−14589

temperature. Time points were taken before each addition of methyl iodide to monitor the reaction progress. After the first five aliquots, the reaction was refluxed at 40 °C, and 10 more aliquots (90-fold excess total) of methyl iodide were added to the reaction while keeping the reaction at 40 °C. Over time the quaternary amine salts precipitated out of solution as a chalky white-gray solid. After the last aliquot was added, the reaction mixture was allowed to stir overnight at room temperature. Following this, the acetone from the reaction mixture was decanted, and the solid was washed with acetone and decanted twice to remove unreacted material. The quaternary amine was dried in the fume hood via a nitrogen stream and dissolved in 50:50:0.1 ACN:H_2O:FA for MS analysis. Iodo-phenyl quaternary amine was synthesized in a manner similar to that of iodo-biphenyl quaternary amine.

Synthesis of (Me-DalPhos)AuCl. Synthesis of the complex was done in accordance to a previously published procedure, with slight modifications (see Scheme 2):[29] In a glovebox with minimal light, 432 mg of Me-DalPhos (1 mmol) and 302 mg (Me_2S)AuCl (1 mmol) were added to a 20 mL scintillation vial equipped with a stir bar and dissolved in 10 mL of DCM. The reaction mixture was then stirred in the dark at room temperature for 2 h. The reaction mixture was filtered through Celite and washed with DCM. All volatiles were removed in vacuo from the filtrate, and the white solid residue was resuspended in hexanes and filtered off on a medium porosity filter frit. The white solid was washed with 5 mL of hexanes and dried under a vacuum to give the desired product. The complex was stored in a glovebox fridge at −20 °C until future use. Spectral data were in good agreement with previous literature. Yield: 600 mg (89.6%).

Scheme 2. Synthesis of (Me-DalPhos)AuCl

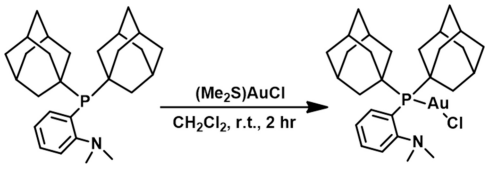

Synthesis of (Me-DalPhos)Au(Aryl)Cl Complexes. At room temperature and open atmosphere, 2 mg of (Me-DalPhos)AuCl was dissolved in 500 μL of DCM. $AgSbF_6$ (1:1 molar ratio) was also dissolved in 250 μL of DCM and was added to the DCM solution containing (Me-DalPhos)AuCl, causing a color change to yellow and formation of a precipitate. Immediately after this, a 250 μL DCM solution containing a 3-fold molar excess of aryl iodide was added to the (Me-DalPhos)AuCl and $AgSbF_6$ solution, causing further color change dependent on the aryl iodide added. Following this, the reaction was allowed to sit for an amount of time ranging from 0.5 to 4 h at room temperature in the dark. Afterward, the DCM solution was removed from the precipitate. Lyophilization of the DCM afforded a yellow-colored solid. As an optional step, this solid was washed sequentially with benzene and *n*-pentane. Both solvents were decanted after each wash step, and the solid was dried again via lyophilization to remove traces of benzene and *n*-pentane. After drying, the solid was dissolved in 1 mL of ACN and was used without further purification.

Modified Synthesis of (Me-DalPhos)Au(Aryl)Cl with Biphenyl Quaternary Amine. The quaternary amine compounds required modifications to the above synthetic protocol. Iodo-biphenyl quaternary amine (BPQA) was dissolved in a solution of $AgSbF_6$ (1:1) in 50:50 ACN:H_2O. A precipitate was formed, and the solution was decanted and lyophilized, affording a white solid. The solid was then dissolved in DCM and the reaction was carried out according to the above procedure with the exception that after addition of all reaction components, the reaction mixture was left to react overnight at 30 °C. To the authors' knowledge, this compound has not been synthesized previously, and NMR and crystal structure data were obtained for (Me-DalPhos)Au-(BPQA)Cl for further characterization of this complex (Figure S10−S13, Table S1). The synthesis of Au-phenyl quaternary amine was carried out in a manner similar to that of Au-biphenyl quaternary amine.

Arylation of Free Thiols with (Me-DalPhos)Au(Aryl)Cl Complexes. All reactions with peptides were performed at room temperature in the dark and allowed to react for 30 min−2 h or as needed to complete the reactions. (Me-DalPhos)Au(Aryl)Cl was added in a 1:1 molar ratio to 50 μL of 215 μM RAAACGVLK in 50:50 ACN:H_2O. Tau fragments were first diluted in ACN to a concentration of 50 μM before adding (Me-DalPhos)Au(Aryl)Cl in a 1:1 ratio. Following the completion of the arylation reaction, an optional liquid−liquid extraction with hexanes was used to remove unwanted side products. Briefly, the reaction mixtures were lyophilized and reconstituted in 200 μL of water with 0.1% FA, and 200 μL of hexanes was added to this. The mixture was then vortexed and centrifuged, and the lower layer (aqueous) was carefully removed by pipet. In the case of the quaternary amine compounds, a liquid−liquid extraction with DCM was performed to remove excess iodo-aryl compound. Following this, the peptides were diluted for direct infusion. For arylation of intact protein, extended reaction times, higher temperature, purified (Me-DalPhos)Au(Aryl)Cl, and increased formic acid content were found to be necessary to denature the protein enough to allow arylation. (Me-DalPhos)Au(Aryl)Cl was added to intact human hemoglobin at a 5:1 molar ratio in 1% FA and 30% ACN by volume. The reaction was allowed to proceed for 2 h at 55 °C, at which point the reaction was removed from heat and diluted for direct infusion.

Photodissociation and Radical-Directed Dissociation Experiments. 266 nm and radical-directed dissociation (RDD) experiments were performed on a Thermo Orbitrap Fusion Lumos with a Crylas FQSS 266-Q3 266 nm laser. Peptides and protein were introduced into the instrument via a nanoflex source from Thermo Scientific. The nanoflex source was modified to allow insertion of a platinum wire into the back of tips pulled from borosilicate glass (Harvard Apparatus GC100T-10). Prior to analysis, peptides were diluted to 5 μM in water with 0.1% FA. Proteins were diluted to 25 μM in water with 0.1% FA. Modified peptides were isolated using the quadrupole prior to 266 nm photodissociation, after which the radical was reisolated for CID and analysis in the Orbitrap mass analyzer. 213 nm photodissociation experiments were performed on a Thermo Orbitrap Velos Pro with a modified HCD cell containing a window allowing pulses from a 213 nm Crylas laser to enter the cell. For the analysis of reaction mixtures and the characterization of (Me-DalPhos)Au(Aryl)Cl complexes, a Thermo LTQ with a modified ion trap allowing irradiation from a 266 nm laser through a quartz window was used. Prior to spraying samples on the LTQ, samples were diluted to 10 μM in 50:50:0.1 ACN:H_2O:FA.

https://doi.org/10.1021/acs.analchem.4c03001
Anal. Chem. 2024, 96, 14581−14589

Scheme 3. Streamlined Workflow for Fast Screening of Aryl Iodide 266 nm PD Yields[a]

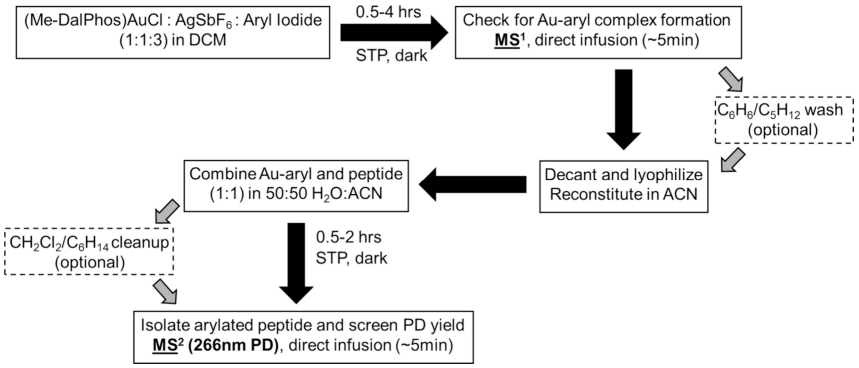

[a]Major steps are indicated by solid boxes. Dashed boxes and gray arrows show steps that were experimentally found to be optional and frequently omitted for the sake of speed. Bold and underlined labels indicate steps utilizing MS^n techniques.

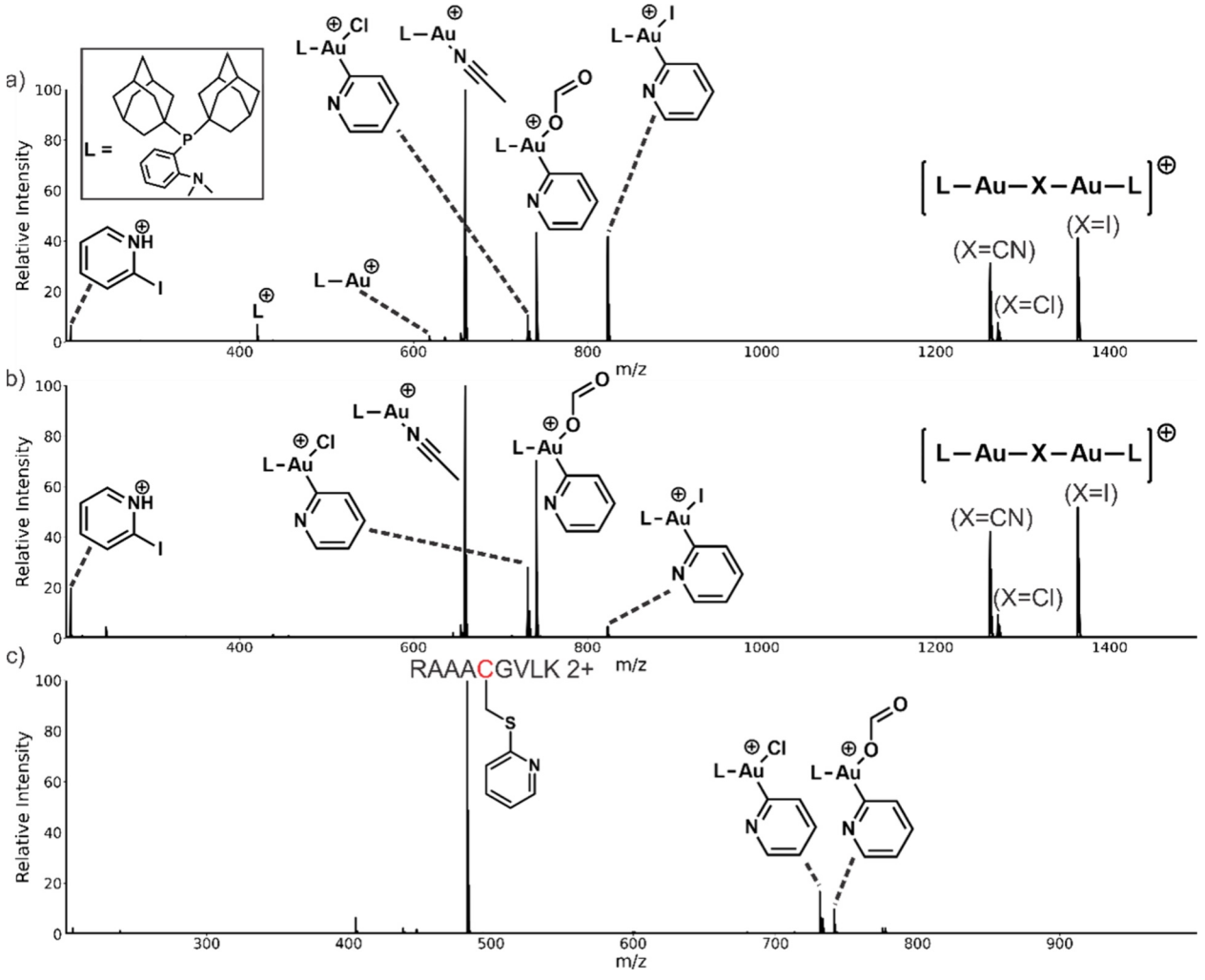

Figure 1. (a) Mass spectrum following synthesis of the 2-pyridyl gold complex and (b) mass spectrum following washes with benzene and pentane. (c) Mass spectrum of modified peptide RAAACGVLK. Unmodified RAAACGVLK (m/z 444) was not found in any significant amount.

Data Analysis. All data were analyzed using Xcalibur (v4.4.16.14). Deconvolution and calculation of fragment ion abundances was performed in FreeStyle (v1.7). For Xtract deconvolution, analyzer type was set to "OT," isotope table was set to "protein," and the relative abundance threshold was set to 1%.

RESULTS AND DISCUSSION

Reaction Chemistry. To maximize the number of chromophores that could be rapidly screened, we modified the original reaction protocols[25] in several ways. First, to utilize the sensitivity afforded by MS analysis, we reduced the scale for each reaction to yield ∼1 mg of product, and reactions were conducted at room temperature and open atmosphere for

https://doi.org/10.1021/acs.analchem.4c03001
Anal. Chem. 2024, 96, 14581−14589

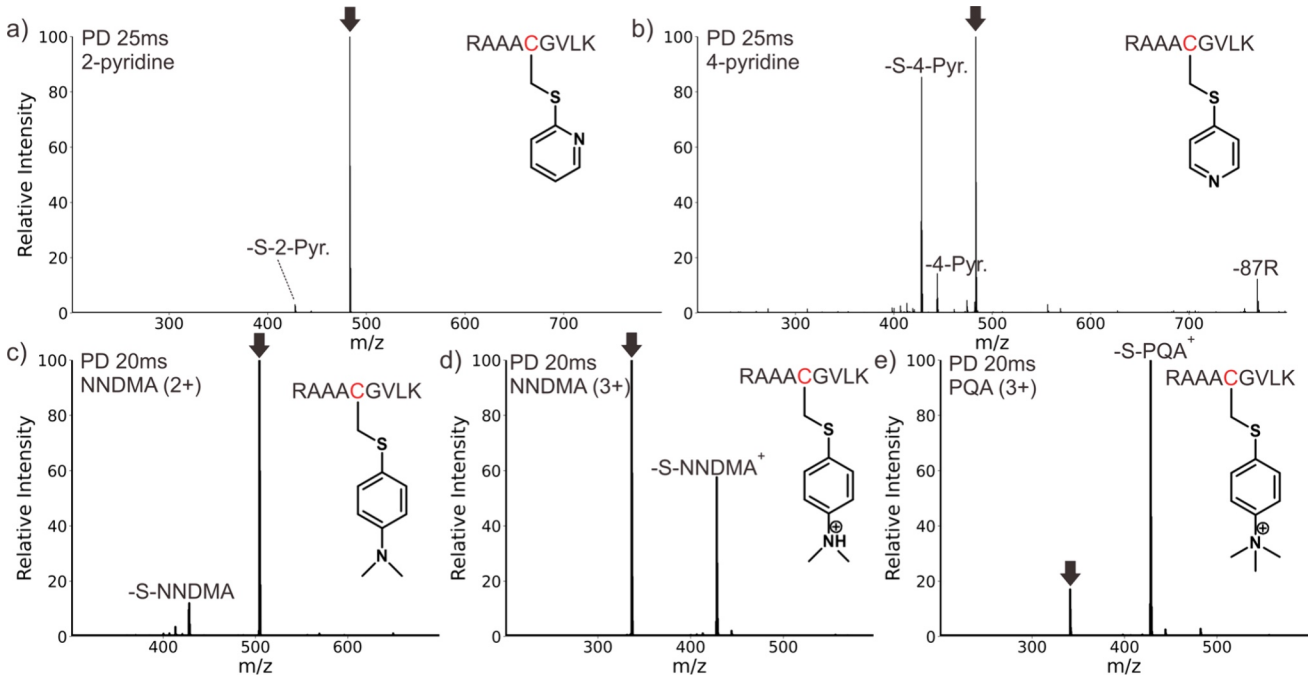

Figure 2. 266 nm Photodissociation spectra for indicated chromophores and PD activation times when measured with a modified RAAACGVLK peptide. Losses are labeled according to aryl group and accompanying atoms, e.g. -S-2-Pyr indicates loss of 2-Pyr and a sulfur atom by homolytic cleavage of the C−S bond. (a) 2-Pyridine, 2+ charge state. (b) 4-Pyridine, 2+ charge state. (c) NNDMA, 2+ charge state. (d) NNDMA, 3+ charge state. PD results in loss of protonated -S-NNDMA. (e) 3+ charge state, PQA. Side chain losses are indicated by the mass loss in Da followed by the identity of the side chain, −87R indicates an ∼87 Da loss from the Arg side chain.

between 30 min and 4 h. Rather than relying on crystallization, we used the isolation capability of the mass spectrometer for purification, and the reaction progress was monitored by taking aliquots from the reaction mixture in real time (Scheme 3). Following observation of the m/z values corresponding to the desired Au-aryl complex, the DCM fraction containing the Au-aryl complex was decanted, lyophilized, and reconstituted in ACN and allowed to react with peptide for between 30 min and 1 h. The reaction products were then isolated and screened for photoyield with 266 nm photoactivation. Following this streamlined workflow, it was possible to obtain arylated peptide from starting materials in as little as 2 h.

During the synthesis of Au-aryl complexes, several interesting side products were observed in the full mass spectrum along with the (Me-DalPhos)Au(Aryl)Cl complex. Figure 1a shows the mass spectrum obtained during the preparation of the 2-pyridyl gold complex. The base peak corresponds to an ACN-adduct of (Me-DalPhos)Au^+. The desired 2-pyridyl-Au(III) complex is also abundant, with the intensity split into three peaks due to combination with chloride, iodide, or formic acid anions. Other significant side products include an apparent Au−Au complex with an anion and (Me-DalPhos)Au^+ dimer bridged by a cyano anion presumably generated by modest breakdown of the solvent ACN. The original protocol included washing the sample with benzene and pentane after synthesis of the (Me-DalPhos)Au-(Aryl)Cl complex, presumably to remove byproducts. Re-examination of the sample after a benzene and pentane wash yielded the results shown in Figure 1b. Although washing appears to favor a shift to the formic acid counterion, the fractional abundance of Au-Aryl products before and after washing was found to be essentially the same (0.26 vs 0.27, compare Figure 1a and 1b). Accordingly, benzene and pentane washes were rarely incorporated into our workflow. Addition of a model peptide (RAAACGVLK) to this reaction mixture (after lyophilization and reconstitution) resulted in nearly 100% modification of the peptide, with some unreacted Au-2-pyridyl left over (Figure 1c). In this case, the amount of unreacted peptide left over after the reaction was almost undetectable. However, lower yields and/or more significant Au byproducts were observed for some of the other chromophores after arylation of peptide (see Figure S1), but in all cases, modification yields were easily sufficient for testing photoactivity. When desirable, liquid−liquid extraction with hexanes and spraying the sample in water with 0.1% formic acid was employed to remove or suppress Au byproducts. This was found to effectively remove most of the competing Au impurities (Figure S2). Interestingly, we found that disulfide formation was also a byproduct of peptide arylation in some cases (Figure S3).

Modification of RAAACGVLK for PD Yield Screening. Having established a streamlined workflow that provides sufficient yield and purity for further experiments, we synthesized a number of (Me-DalPhos)Au(Aryl)Cl complexes and used them to arylate RAAACGVLK. Illustrative results from PD experiments are shown in Figure 2 (additional PD spectra for all chromophores tested are available in Figure S4 of the Supporting Information). For example, in Figure 2a, very little PD is observed for 2-pyridine, while significantly better PD is observed for 4-pyridine in Figure 2b. Given the expected similar electronic properties for para- versus ortho-substituted pyridinal groups, the strikingly different PD yields illustrate that results may not be easily predictable by standard chemical intuition. Although hydrogen bonding or charge proximity has been noted to interfere with PD yields in past experiments,[30] results obtained for N,N-dimethylaniline (NNDMA) reveal the opposite trend for C−S bond cleavage. The PD yield for neutral NNDMA is ∼16% after 20 ms of 266

https://doi.org/10.1021/acs.analchem.4c03001
Anal. Chem. 2024, 96, 14581−14589

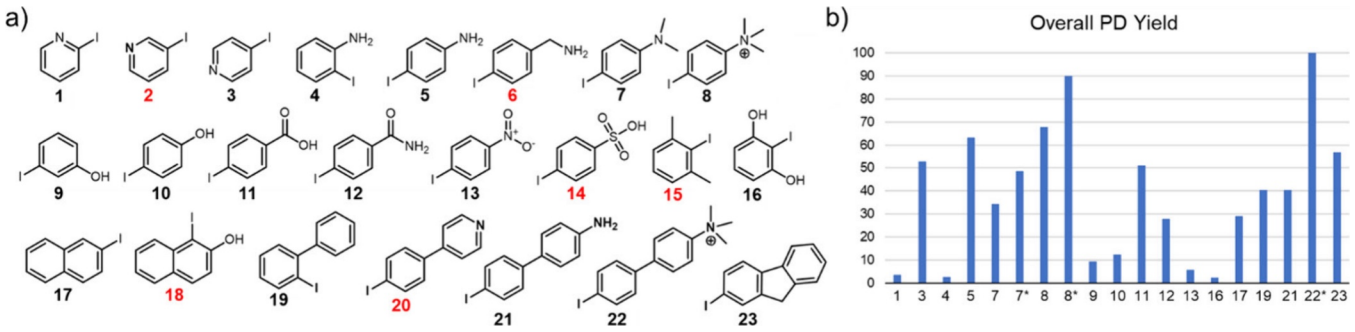

Figure 3. (a) Selection of aryl iodides tested. Red numbers indicate aryl iodides that were not able to be incorporated into (Me-DalPhos)Au(Aryl)Cl complexes, and thus were not able to be tested for PD yield. (b) Overall PD yield for modified RAAACGVLK. The overall PD yield was calculated as (1-Precursor FRAB) x 100 with 20 ms activation time. *indicates 20 ms MS^2 266 nm PD data obtained on 3+ charge states of arylated RAAACGVLK.

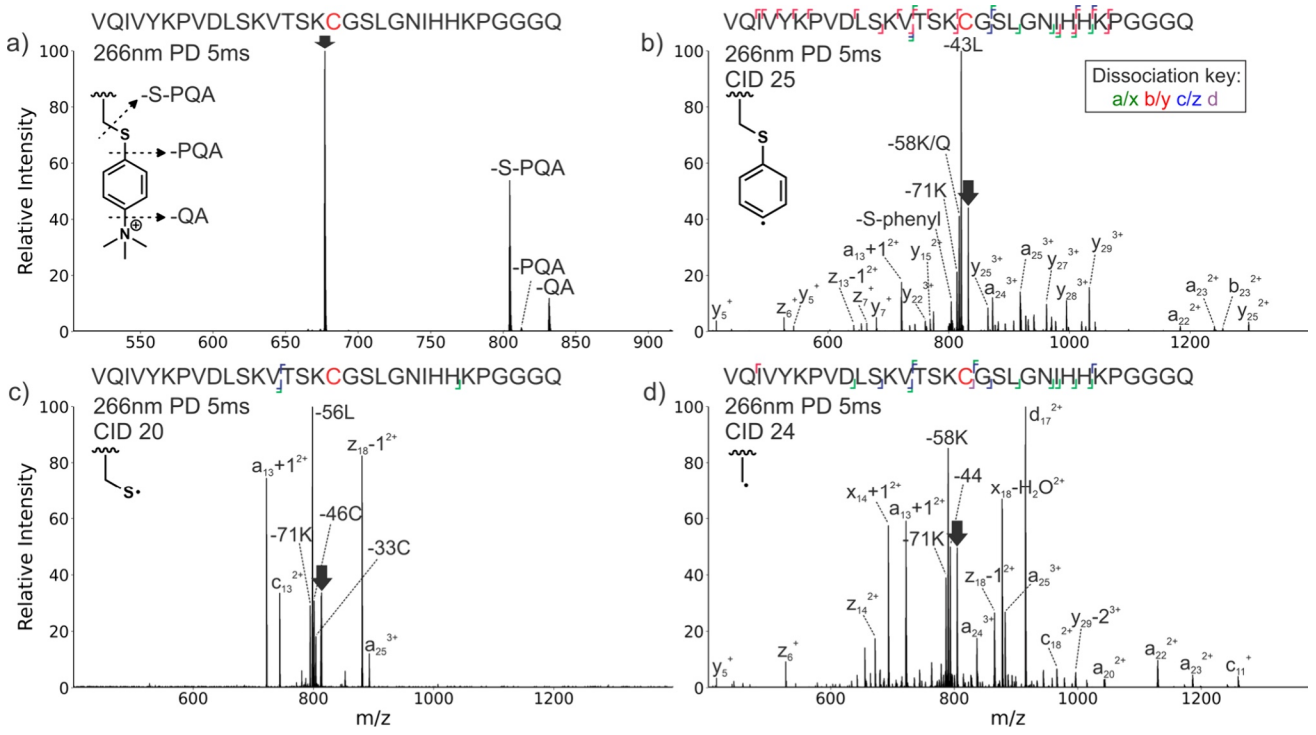

Figure 4. (a) 266 nm PD on a tau peptide modified with PQA, producing indicates losses by homolytic cleavage. RDD on radicals formed during PD on tau-derived VQIV peptide modified with PQA, (b) phenyl radical, (c) thiyl radical, and (d) beta radical. Side chain losses are indicated by the mass loss in Da followed by the identity of the side chain.

nm activation (Figure 2c). For the 3+ charge state, where the modification is protonated, the PD yield increases to ∼63%. Note that protonation of the NNDMA is confirmed by a reduction in charge of the peptide after photodissociation (i.e., all detectable products are now at higher m/z after mass loss rather than lower m/z). To further explore the effect of charge on the aryl group, NNDMA was methylated to produce phenyl quaternary amine (PQA). For PQA, the PD yield improves further to ∼83%. Again, it is difficult to rationalize why the quaternary nitrogen outperforms the protonated nitrogen, emphasizing the importance of the capability to rapidly screen a large number of candidate structures to obtain an optimal performance.

To facilitate comparison of PD yields among all aryl groups tested (Figure 3a), we calculated the fractional abundance of the precursor in the MS^2 spectra at 20 ms and subtracted this from the total ion count for each spectrum. Therefore, a value of 100 in Figure 3b indicates nearly complete dissociation of the precursor or a high PD yield. Fixed charge-containing compounds 8 and 22 were found to exhibit the highest overall PD yield. The primary products for all chromophores in Figure 3b result from C−S bond cleavage between the methylene carbon and the sulfur atom in the Cys side chain. Nominally, this yields a beta radical immediately following the excited-state dissociation, but it is apparent that this radical can rapidly migrate (as is required to generate the −87R arginine side chain loss in Figure 2b). Additionally, although most of our experiments were performed at 266 nm, we also tested some chromophores for the PD yield at 213 nm. Some aryl groups were found to exhibit greater PD yields at 213 nm than at 266 nm, while others exhibited noticeably worse PD yields at 213 nm, showing that chromophore selection may change significantly depending on which wavelength is used (Figure S5).

https://doi.org/10.1021/acs.analchem.4c03001
Anal. Chem. 2024, 96, 14581−14589

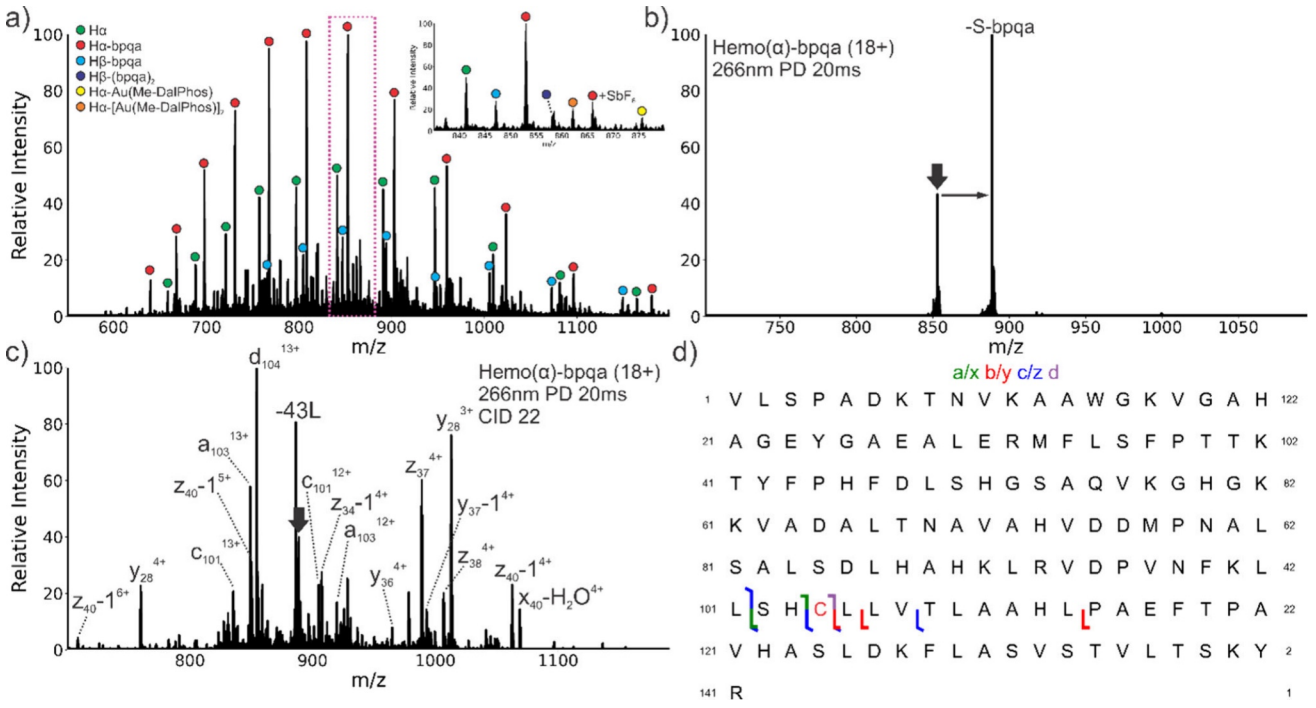

Figure 5. Modification of human hemoglobin with biphenyl quaternary amine (BPQA). (a) Spectrum of the modified protein with inset showing a zoomed-in view of m/z 835−880. (b) 266 nm PD on the 18+ charge state of arylated hemo-α, 20 ms activation time. (c) RDD spectrum of 18+ hemo-α. (d) Fragmentation map for hemo-α showing cleavage is localized to the site of modification. a/x fragments are shown in green, b/y in red, c/z in blue, and d in purple. Side chain losses are indicated by the mass loss in Da followed by the identity of the side chain.

Radical-Directed Dissociation. To explore the utility of radicals created with this approach, we conducted RDD experiments with select chromophores on more complicated peptides. Although BPQA provided the greatest photoyield, some of the most interesting results were obtained with PQA, which produces three different radicals (Figure 4a) in yields sufficient for subsequent collisional activation when coupled to the tau-derived sequence VQIVYKPVDL SKVTSKCGSL GNIHHKPGGG Q (VQIV for short). The radicals derive from homolytic cleavage at either the β-C−S bond, the phenyl-C−S bond, or the C−N bond of the quaternary amine. To explore the results of RDD on these different PD products, each of these radicals were isolated and collisionally activated (Figure 4b-d). Activation of the phenyl radical produced a variety of backbone fragments, as well as abundant leucine and lysine side chain losses (Figure 4b). The −43L side chain loss seems to be the most abundant radical dissociation pathway for this species, which is not surprising given that Leucine is prone to undergo side chain losses during RDD[14] and is only three residues away from the arylated Cysteine. Additional information about the behavior of this radical is given by the significant number of a- and z-ions, indicating that the phenyl radical migrates easily to a variety of different locations on the peptide backbone before initiating fragmentation. The presence of b/y ions also suggests that some low-energy mobile proton-initiated fragmentation pathways also exist. In contrast, activation of the thiyl radical produced much more specific fragmentation, including an abundant a_{13}+1 and z_{18}−1 complementary pair (Figure 4c). This fragment pair is located between Val13 and Thr14, consistent with previous observations that a+1 and z−1 pairs are often observed at Ser/Thr residues during RDD.[14] In addition, new side chain losses are observed including −56L, −46C, and −33C. The latter two Cys-specific side chain losses do not appear in the RDD spectra for the other radicals and would seem to be more favorable in this case due to the radical's unique positioning. These losses have also been observed in other systems involving thiyl radicals.[31] These results indicate that not surprisingly radical migration is more restricted for the less active thiyl radical relative to the phenyl radical. RDD on the beta radical product yields a spectrum that is also dissimilar to the other two RDD spectra (Figure 4d). Specific a+1 and z−1 fragments are observed again at Val13/Thr14, but an even more abundant d_{17}/x_{14} complementary pair is observed at the modified Cys. The d_{17} and x_{14} fragments result from backbone attack by the original beta radical, which appears to resist immediate migration for this peptide and charge state. d-Ions located at the site of the arylated cysteine are consistent with the previous 266 nm PD data on modified Cys.[18,22] Similar results were obtained when RDD was performed on the same peptide modified with BPQA (compare Figure 4d and Figure S6), although in this case only the beta radical was available for RDD. Overall, these results show that the initial location and type of radical produced during photoactivation can significantly affect the subsequent RDD fragmentation that is ultimately observed. In addition to this example, data illustrating RDD for several sequences were also obtained (see SI Figures S6−S8).

To test whether intact proteins can also be effectively arylated, we attempted to modify human hemoglobin with biphenylquaternary amine (**22,** BPQA). Alpha hemoglobin (α-hemo) contains a single free thiol at Cys105, while β-hemo contains two free thiols at Cys94 and Cys113. While peptides are often structurally disordered, with most side chains exposed to bulk solvent, proteins are more complicated due to the folded structures they adopt, which can impair side chain accessibility. In order to achieve the maximum modification efficiency, we found it necessary to heat a

https://doi.org/10.1021/acs.analchem.4c03001
Anal. Chem. 2024, 96, 14581−14589

reaction mixture of 1:5 protein:Au-BPQA at 55 °C for 2 h. In addition, a high-purity, recrystallized sample of Au-BPQA was employed to reduce the level of formation of side products. The optimized results are shown in Figure 5a. The most intense peaks correspond to arylated α-hemo, although some unreacted α-hemo was still present after 2 h of reaction time (Figure 5a, red and green labels). In addition, single- and double-arylated β-hemo groups are also observed (Figure 5a, light blue and dark blue labels). Minor additional peaks are also observed, such as adducted Au(Me-DalPhos) (Figure 5a inset, yellow and orange labels; see Figure S9 for the structure). Although intact proteins are more demanding to modify than smaller peptides, our results show that it is possible to achieve high yields with a few extra precautions.

After successfully modifying intact hemoglobin, we next explored the PD behavior. Examination of the largely unfolded 18+ charge state for 20 ms of activation time at 266 nm produced a high PD yield (Figure 5b). Interestingly, the PD yield at 20 ms for BPQA-modified RAAACGVLK was much higher, resulting in complete depletion of the precursor (see Figure S4r). This discrepancy in PD yields between peptide and intact protein may be attributed to homolytic cleavage without loss of BPQA or to reduced absorption, which could both result from interactions with negatively charged side chains elsewhere on the protein. To explore these possibilities further, PD was performed on higher charge states of α-hemo-BPQA. At higher charge states, negatively charged sites in the protein are less likely to be present. Significant increases in PD yield were observed at charge states >21+ (Figure S14).

Following 266 nm PD, the radical was reisolated and activated with CID, producing abundant a-, c-, z-, x-, and y-ions (Figure 5c). Notably, an abundant d−z pair is observed at Cys105 from dissociation of the original beta radical. In addition, leucine side chain loss is abundant as well as an abundant y28 ion. An abundant y28 ion is also observed when the 18+ charge state of BPQA-modified α-hemo is fragmented with CID in the absence of any PD (Figure S15), suggesting that this ion likely originates from the proline effect. Mapping of the fragments reveals that most of the radical-based fragmentation occurs near the arylated Cys105 with only the (proton-initiated) y28 fragment occurring farther away in the sequence (Figure 5d). These results suggest that RDD on arylated intact proteins can in some cases produce very specific fragmentation near the site of modification. In addition to α-hemo, PD and RDD data were also collected on the single arylation of β-hemo. 266 nm PD (40 ms) produced loss of -S-BPQA during PD (Figure S16). RDD on β-hemo produced a spectrum with very few radical fragments, being dominated mostly by b/y-ions resulting from mobile proton-driven fragmentation (Figure S17). A few z-ions located near Cys113 identify this Cysteine as the most likely site of modification. A potential explanation for the abundance of b/y fragments and lack of radical-based fragments is that the radical is largely sequestered after formation at Cys113 by Cys94, resulting in little to no radical migration. This is supported by the fact that there are only a small number of z-ions localized near Cys113. Overall, thiol-selective Au(III) chemistry seems to be well-suited for modification of intact proteins with the caveat that denaturing reaction conditions are required due to the influence of a higher order protein structure, indicating that arylation of proteins is more difficult than peptides. In the course of these experiments, we also arylated intact SOD1 (containing a free thiol near the N-terminus) and found that similar denaturing conditions were required for this protein as well (Figure S8). In the case of proteins that are more intrinsically disordered, Cys arylation via Au(III) chemistry would likely be much more straightforward and may not require the denaturing conditions used for hemoglobin. In any case, Cys arylation provides yet another useful handle for introducing a 266 nm-cleavable radical precursor for RDD on intact proteins.

CONCLUSION

In this work, we characterized the 266 nm photoactivity of various arylated Cys residues by streamlining a workflow that could combine the separation and sensitivity afforded by mass spectrometry with a previously reported Au(III)-based modification strategy. Surprisingly, our chromophore screening revealed that aryls with fixed charges (such as PQA and BPQA) were the most efficient at cleaving carbon−sulfur bonds upon photoactivation. If these chromophores follow previous trends where solution and gas-phase absorption were found to be similar,[12] our work could provide a useful starting point for those interested in developing condensed-phase applications. Although peptide modification proved to be quite straightforward, arylation of intact proteins was found to be more complicated due to the presence of a tertiary structure and an increased propensity for off-target side reactions. Nevertheless, high yields were still obtainable with slightly modified reaction procedures. For all classes of molecules tested, from small peptides to large proteins, arylation was highly specific to Cys residues and photoactivation at 266 nm produced radical species that could be further activated with collisions to reveal information about sequence and structure. The combination of chemical synthesis for installing useful modifications that enhance mass spectrometric analyses, particularly for intact proteins, appears to be an area that holds great promise for the future .

ASSOCIATED CONTENT

Supporting Information

The Supporting Information is available free of charge at https://pubs.acs.org/doi/10.1021/acs.analchem.4c03001.

Additional mass spectra of arylated peptides and proteins; PD and RDD spectra; chemical structure for $[Au(Me\text{-}DalPhos)]_2$ byproduct; NMR spectra and crystal structure of (Me-DalPhos)Au(BPQA)Cl; CID spectrum of arylated 18+ hemoglobin alpha; supplemental methods for NMR sample preparation and crystal growth (PDF)

AUTHOR INFORMATION

Corresponding Author

Ryan R. Julian − *Department of Chemistry, University of California, Riverside, California 92521, United States;* orcid.org/0000-0003-1580-8355; Email: ryan.julian@ucr.edu

Authors

Jacob W. Silzel − *Department of Chemistry, University of California, Riverside, California 92521, United States*

Chengwei Chen − *Department of Chemistry, University of California, Riverside, California 92521, United States*

Colomba Sanchez-Marsetti − *Department of Chemistry, University of California, Riverside, California 92521, United States;* orcid.org/0009-0008-5368-2056
Phillip Farias − *Department of Chemistry, University of California, Riverside, California 92521, United States*
Veronica Carta − *Department of Chemistry, University of California, Riverside, California 92521, United States;* orcid.org/0000-0001-8089-8436
W. Hill Harman − *Department of Chemistry, University of California, Riverside, California 92521, United States;* orcid.org/0000-0003-0400-2890

Complete contact information is available at: https://pubs.acs.org/10.1021/acs.analchem.4c03001

Notes

The authors declare no competing financial interest.

■ ACKNOWLEDGMENTS

The authors would like to thank John Syka, Chris Mullen, and Josh Hinkle from Thermo Fisher Scientific for valuable discussions and assistance with instrument modifications, as well as the NSF for funding (RRJ for CHE-1904577 and WHH for CHE-1752876).

■ REFERENCES

(1) Julian, R. R. *J. Am. Soc. Mass Spectrom.* **2017**, *28* (9), 1823−1826.
(2) Brodbelt, J. S.; Morrison, L. J.; Santos, I. *Chem. Rev.* **2020**, *120* (7), 3328−3380.
(3) Fornelli, L.; Srzentić, K.; Toby, T. K.; Doubleday, P. F.; Huguet, R.; Mullen, C.; Melani, R. D.; dos Santos Seckler, H.; DeHart, C. J.; Weisbrod, C. R.; Durbin, K. R.; Greer, J. B.; Early, B. P.; Fellers, R. T.; Zabrouskov, V.; Thomas, P. M.; Compton, P. D.; Kelleher, N. L. *Mol. Cell. Proteomics* **2020**, *19* (2), 405−420.
(4) Shaw, J. B.; Li, W.; Holden, D. D.; Zhang, Y.; Griep-Raming, J.; Fellers, R. T.; Early, B. P.; Thomas, P. M.; Kelleher, N. L.; Brodbelt, J. S. *J. Am. Chem. Soc.* **2013**, *135* (34), 12646−12651.
(5) Bonner, J.; Talbert, L. E.; Akkawi, N.; Julian, R. R. *Analyst* **2018**, *143* (21), 5176−5184.
(6) Quick, M. M.; Crittenden, C. M.; Rosenberg, J. A.; Brodbelt, J. S. *Anal. Chem.* **2018**, *90* (14), 8523−8530.
(7) Lanzillotti, M.; Brodbelt, J. S. *J. Am. Soc. Mass Spectrom.* **2023**, *34* (2), 279−285.
(8) Zhang, L.; Reilly, J. P. *Anal. Chem.* **2010**, *82* (3), 898−908.
(9) Girod, M.; Sanader, Z.; Vojkovic, M.; Antoine, R.; MacAleese, L.; Lemoine, J.; Bonacic-Koutecky, V.; Dugourd, P. *J. Am. Soc. Mass Spectrom.* **2015**, *26* (3), 432−443.
(10) Aponte, J. R.; Vasicek, L.; Swaminathan, J.; Xu, H.; Koag, M. C.; Lee, S.; Brodbelt, J. S. *Anal. Chem.* **2014**, *86* (13), 6237−6244.
(11) Wäldchen, F.; Becher, S.; Esch, P.; Kompauer, M.; Heiles, S. *Analyst.* **2017**, *142* (24), 4744−4755.
(12) Ly, T.; Zhang, X.; Sun, Q.; Moore, B.; Tao, Y.; Julian, R. R. *Chem. Commun.* **2011**, *47*, 2835−2837.
(13) Silzel, J. W.; Julian, R. R. *J. Am. Soc. Mass Spectrom.* **2023**, *34* (3), 452−458.
(14) Sun, Q.; Nelson, H.; Ly, T.; Stoltz, B. M.; Julian, R. R. *J. Proteome Res.* **2009**, *8* (2), 958−966.
(15) Tao, Y.; Quebbemann, N. R.; Julian, R. R. *Anal. Chem.* **2012**, *84* (15), 6814−6820.
(16) Lambeth, T. R.; Julian, R. R. *J. Am. Soc. Mass Spectrom.* **2022**, *33* (8), 1338−1345.
(17) Ly, T.; Julian, R. R. *J. Am. Chem. Soc.* **2008**, *130*, 351−358.
(18) Diedrich, J. K.; Julian, R. R. *J. Am. Chem. Soc.* **2008**, *130* (37), 12212−12213.
(19) Osburn, S.; Berden, G.; Oomens, J.; O'Hair, R. A. J.; Ryzhov, V. *J. Am. Soc. Mass Spectrom.* **2012**, *23* (6), 1019−1023.
(20) Nauser, T.; Casi, G.; Koppenol, W. H.; Schöneich, C.; Schoeneich, C. *J. Phys. Chem. B* **2008**, *112* (47), 15034−15044.
(21) Miseta, A.; Csutora, P. *Mol. Biol. Evol.* **2000**, *17* (8), 1232−1239.
(22) Diedrich, J. K.; Julian, R. R. *Anal. Chem.* **2010**, *82* (10), 4006−4014.
(23) Vinogradova, E. V.; Zhang, C.; Spokoyny, A. M.; Pentelute, B. L.; Buchwald, S. L. *Nature* **2015**, *526* (7575), 687−691.
(24) Jbara, M.; Maity, S. K.; Brik, A. *Angew. Chem., Int. Ed.* **2017**, *56*, 10644−10655.
(25) Messina, M. S.; Stauber, J. M.; Waddington, M. A.; Rheingold, A. L.; Maynard, H. D.; Spokoyny, A. M. *J. Am. Chem. Soc.* **2018**, *140* (23), 7065−7069.
(26) Doud, E. A.; Tilden, J. A. R.; Treacy, J. W.; Chao, E. Y.; Montgomery, H. R.; Kunkel, G. E.; Olivares, E. J.; Adhami, N.; Kerr, T. A.; Chen, Y.; Rheingold, A. L.; Loo, J. A.; Frost, C. G.; Houk, K. N.; Maynard, H. D.; Spokoyny, A. M. *J. Am. Chem. Soc.* **2024**, *146* (18), 12365−12374.
(27) Montgomery, H. R.; Messina, M. S.; Doud, E. A.; Spokoyny, A. M.; Maynard, H. D. *Bioconjugate Chem.* **2022**, *33* (8), 1536−1542.
(28) Stauber, J. M.; Rheingold, A. L.; Spokoyny, A. M. *Inorg. Chem.* **2021**, *60* (7), 5054−5062.
(29) Zhang, S.; Wang, C.; Ye, X.; Shi, X. *Angew. Chem., Int. Ed.* **2020**, *59*, 20470.
(30) Kirk, B. B.; Trevitt, A. J.; Blanksby, S. J.; Tao, Y.; Moore, B. N.; Julian, R. R. *J. Phys. Chem. A* **2013**, *117* (6), 1228−1232.
(31) Lam, A. K. Y.; Ryzhov, V.; O'Hair, R. A. J. *J. Am. Soc. Mass Spectrom.* **2010**, *21* (8), 1296−1312.